UNIVERSITYOF BIRMINGHAM

Search for CP violation using T-odd correlations in $D^0 \to$ K$^+$K$^-\pi^+\pi^-$decays

LHCb Collaboration; Aaij, R.; Adeva, B.; Adinolfi, M.; Affolder, A.; Ajaltouni, Z.; Akar, S.; Albrecht, J.; Alessio, F.; Alexander, M.; Ali, S.; Alkhazov, G.; Alvarez Cartelle, P.; Alves, A. A.; Amato, S.; Amerio, S.; Amhis, Y.; An, L.; Anderlini, L.; Anderson, J.

[Link to publication on Research at Birmingham portal](#)

Search for CP violation using T-odd correlations in $D^0 \to K^+K^-\pi^+\pi^-$ decays

The LHCb collaboration

E-mail: nicola.neri@mi.infn.it

ABSTRACT: A search for CP violation using T-odd correlations is performed using the four-body $D^0 \to K^+K^-\pi^+\pi^-$ decay, selected from semileptonic B decays. The data sample corresponds to integrated luminosities of $1.0\,\text{fb}^{-1}$ and $2.0\,\text{fb}^{-1}$ recorded at the centre-of-mass energies of $7\,\text{TeV}$ and $8\,\text{TeV}$, respectively. The CP-violating asymmetry $a_{CP}^{T\text{-odd}}$ is measured to be $(0.18 \pm 0.29\,(\text{stat}) \pm 0.04\,(\text{syst}))\%$. Searches for CP violation in different regions of phase space of the four-body decay, and as a function of the D^0 decay time, are also presented. No significant deviation from the CP conservation hypothesis is found.

Contents

1 Introduction

Violation of the CP symmetry in charm decays is expected to be very small in the Standard Model (SM) [1, 2], however, asymmetries at a few times 10^{-3} within the SM cannot be excluded according to recent calculations [3–5]. A significant excess of CP violation (CPV) with respect to the theoretical predictions would be a signature of physics beyond the SM. The study of CPV in singly Cabibbo-suppressed charm decays is uniquely sensitive to physics beyond the SM, in particular through new contributions in strong penguin and chromomagnetic dipole operators [2]. The analysis of singly Cabibbo-suppressed $D^0 \to K^+K^-\pi^+\pi^-$[1] decays allows localised CPV in different regions of phase space to be probed. This approach enhances the sensitivity due to several interfering amplitudes with different relative strong phases contributing to the decay.

The analysis in ref. [6] quotes a p-value of 9.1% for the compatibility with the CP conservation hypothesis, using D^*-tagged promptly-produced D^0 mesons. In the present analysis, a sample of $D^0 \to K^+K^-\pi^+\pi^-$ decays, selected from semileptonic B decays, is used to measure a CP-violating parameter based on T-odd correlations characterised by different sensitivity to CPV [7, 8]. Using triple products of final state particle momenta in the D^0 centre-of-mass frame, $C_T \equiv \vec{p}_{K^+} \cdot (\vec{p}_{\pi^+} \times \vec{p}_{\pi^-})$ for D^0 and $\overline{C}_T \equiv \vec{p}_{K^-} \cdot (\vec{p}_{\pi^-} \times \vec{p}_{\pi^+})$ for $\bar{D}^0$ decays, two T-odd observables,

$$A_T \equiv \frac{\Gamma_{D^0}(C_T > 0) - \Gamma_{D^0}(C_T < 0)}{\Gamma_{D^0}(C_T > 0) + \Gamma_{D^0}(C_T < 0)}, \qquad \overline{A}_T \equiv \frac{\Gamma_{\bar{D}^0}(-\overline{C}_T > 0) - \Gamma_{\bar{D}^0}(-\overline{C}_T < 0)}{\Gamma_{\bar{D}^0}(-\overline{C}_T > 0) + \Gamma_{\bar{D}^0}(-\overline{C}_T < 0)}, \quad (1.1)$$

---

[1]Throughout this paper the use of charge conjugate reactions is implied, unless otherwise indicated.

can be studied [9], where Γ_{D^0} ($\Gamma_{\bar{D}^0}$) is the partial decay width of D^0 ($\bar{D}^0$) decays to $K^+K^-\pi^+\pi^-$ in the indicated C_T ($\overline{C}_T$) range. However, because final state interaction (FSI) effects could introduce fake asymmetries [9, 10], these are not theoretically clean CP-violating observables. A well defined CP-violating observable is

$$a_{CP}^{T\text{-odd}} \equiv \frac{1}{2}(A_T - \overline{A}_T), \tag{1.2}$$

as FSI effects cancel out in the difference. In contrast to the asymmetry between the phase-space integrated rates in a $D^0 \to V_1 V_2$ decay (where V_i indicates a vector meson), $a_{CP}^{T\text{-odd}}$ is sensitive to CP violation in interference between even- and odd- partial waves of the $V_1 V_2$ system [7].

Previous measurements of $a_{CP}^{T\text{-odd}}$ are compatible with no CPV: FOCUS measured $a_{CP}^{T\text{-odd}} = (1.0 \pm 5.7 \pm 3.7)\%$ [11], and BaBar measured $a_{CP}^{T\text{-odd}} = (0.10 \pm 0.51 \pm 0.44)\%$ [12]. The physics observables, A_T, $\overline{A}_T$, and $a_{CP}^{T\text{-odd}}$ are by construction insensitive to $D^0/\bar{D}^0$ production asymmetries, detector- and reconstruction-induced charge asymmetries. The measurement described in this paper determines the CP-violating observable $a_{CP}^{T\text{-odd}}$ with an improved precision. For the first time, $a_{CP}^{T\text{-odd}}$ is measured in different regions of phase space and in bins of D^0 decay time, allowing to probe for CP violation both in the decay amplitude and in its interference with the mixing amplitude.

2 Detector

The LHCb detector [13] is a single-arm forward spectrometer covering the pseudorapidity range $2 < \eta < 5$, designed for the study of particles containing b or c quarks. The detector includes a high-precision tracking system consisting of a silicon-strip vertex detector surrounding the pp interaction region [14], a large-area silicon-strip detector located upstream of a dipole magnet with a bending power of about $4\,\mathrm{Tm}$, and three stations of silicon-strip detectors and straw drift tubes [15] placed downstream of the magnet. The tracking system provides a measurement of momentum, p, with a relative uncertainty that varies from 0.4% at low momentum to 0.6% at $100\,\mathrm{GeV}/c$. The minimum distance of a track to a primary vertex, the impact parameter, is measured with a resolution of $(15 + (29\,\mathrm{GeV}/c)/p_\mathrm{T})\,\mu\mathrm{m}$, where p_T is the component of p transverse to the beam. Different types of charged hadrons are distinguished using information from two ring-imaging Cherenkov (RICH) detectors [16]. Photon, electron and hadron candidates are identified by a calorimeter system consisting of scintillating-pad and preshower detectors, an electromagnetic calorimeter and a hadronic calorimeter. Muons are identified by a system composed of alternating layers of iron and multiwire proportional chambers [17]. The trigger [18] consists of a hardware stage, based on information from the calorimeter and muon systems, followed by a software stage, which applies a full event reconstruction.

Events are required to pass both hardware and software trigger selections. The software trigger identifies $D^0 \to K^+K^-\pi^+\pi^-$ (signal) and $D^0 \to K^-\pi^+\pi^-\pi^+$ (control sample) events from $B \to D^0\mu^-X$ decays, where X indicates any system composed of charged and neutral particles, by requiring a four-track secondary vertex with a scalar sum of p_T of the tracks

greater than $1.8\,\mathrm{GeV}/c$. The D^0 daughter tracks are required to have $p_{\mathrm{T}} > 0.3\,\mathrm{GeV}/c$ and momentum $p > 2\,\mathrm{GeV}/c$. The muon track is selected with $p_{\mathrm{T}} > 1.2\,\mathrm{GeV}/c$ and $p > 2\,\mathrm{GeV}/c$. Tracks have to be compatible with detached decay vertices of B and D^0 decays. Therefore, a requirement is imposed for all the tracks in the signal candidate on the χ^2_{IP}, i.e. the difference in χ^2 of a given primary vertex reconstructed with and without the considered particle, to be greater than 9. The invariant mass of the $D^0\mu$ system is required to be less than $6.2\,\mathrm{GeV}/c^2$.

In the simulation, pp collisions are generated using PYTHIA [19, 20] with a specific LHCb configuration [21]. Decays of hadronic particles are described by EVTGEN [22]. The interaction of the generated particles with the detector and its response are implemented using the GEANT4 toolkit [23, 24] as described in ref. [25].

3 Selection

The analysis is based on data recorded by the LHCb experiment, at center-of-mass energies of 7 TeV and 8 TeV, corresponding to integrated luminosities of $1.0\,\mathrm{fb}^{-1}$ and $2.0\,\mathrm{fb}^{-1}$, respectively.

The D^0 candidates are formed from combinations of kaon and pion candidate tracks and then combined with a muon candidate track to reconstruct the semileptonic B decay. The flavour of the D^0 is identified by the charge of the muon, i.e. a negative charge identifies a D^0 meson and a positive charge identifies a $\bar{D}^0$ meson. The information from the RICH system is used to distinguish between kaons and pions, while the information from the muon system is used to identify muon candidates. The D^0 meson decay vertex is required to be downstream of the B decay vertex. The invariant mass of the $D^0\mu$ system is required to be in the range $[2.6, 5.2]\,\mathrm{GeV}/c^2$.

Two main sources of peaking background in $m(K^+K^-\pi^+\pi^-)$, the reconstructed invariant mass of D^0 candidates, are present and consist of $D^0 \to K^0_S K^+K^-$ decays, and $D^0 \to K^+K^-\pi^+\pi^-$ decays from D^0 mesons that originate at the interaction point, referred to as "prompt" charm decays in the following. The small component of $D^0 \to K^0_S K^+K^-$ events is vetoed by requiring the invariant mass of the $\pi^+\pi^-$ system to be more than 3σ away from the known K^0_S mass [26], where $\sigma = 4.5\,\mathrm{MeV}/c^2$ is the resolution determined from the fit to data. The contribution of prompt charm decays is estimated by fitting the distribution of the logarithm of the χ^2_{IP} of the D^0 meson. The prompt component and the signal component from semileptonic B decays accumulate at 0 and at 5, respectively. The fraction of prompt D^0 decays in our sample is measured to be $f_{\mathrm{prompt}} = (1.20 \pm 0.08)\%$ and the effect of its presence is accounted for as a systematic uncertainty. The distributions of D^0 decays where pions and kaons have not been correctly identified have been studied and do not peak in $m(K^+K^-\pi^+\pi^-)$. When multiple candidates are reconstructed, one candidate per event is retained, by random choice. This happens in 0.7% of the events. The signal yield for $D^0 \to K^+K^-\pi^+\pi^-$ from $B \to D^0\mu^-X$ decays, obtained from an extended maximum likelihood fit to the $m(K^+K^-\pi^+\pi^-)$ distribution, is $(171.3 \pm 0.6) \times 10^3$ events with a sample purity of about 75%.

Sample	Signal Decays
$D^0,\quad C_T > 0$	$39\,628 \pm 256$
$D^0,\quad C_T < 0$	$45\,762 \pm 272$
$\bar{D}^0,\ -\overline{C}_T > 0$	$39\,709 \pm 256$
$\bar{D}^0,\ -\overline{C}_T < 0$	$46\,162 \pm 274$

Table 1. Number of signal decays obtained from the fit to data for each of the four samples defined by the $D^0/\bar{D}^0$ flavour and the sign of C_T or $\overline{C}_T$.

By using identical kinematic selection criteria as for the signal, Cabibbo-favoured $D^0 \to K^-\pi^+\pi^-\pi^+$ decays are also reconstructed with a signal yield of about of 6.211×10^6 and a purity of about 95%. These decays are used for control checks and for assessing systematic uncertainties.

4 Asymmetry measurements

The selected data sample is split into four subsamples according to the charge of the muon candidate, which determines the flavour of the D^0, and the sign of C_T ($\overline{C}_T$). The reconstruction efficiencies are equal, within their uncertainties, for $C_T > 0$ ($-\overline{C}_T > 0$) and for $C_T < 0$ ($-\overline{C}_T < 0$) according to studies based on simulated events and on the $D^0 \to K^-\pi^+\pi^-\pi^+$ control sample. A simultaneous maximum likelihood fit to the $m(K^+K^-\pi^+\pi^-)$ distribution of the four subsamples is used to determine the number of signal and background events, and the asymmetries A_T and $\overline{A}_T$. The fit model consists of two Gaussian functions with common mean for the signal and an exponential function for the background. The two asymmetries A_T and $\overline{A}_T$ are included in the fit model as

$$
\begin{aligned}
N_{D^0, C_T > 0} &= \frac{1}{2} N_{D^0}(1 + A_T), \\
N_{D^0, C_T < 0} &= \frac{1}{2} N_{D^0}(1 - A_T), \\
N_{\bar{D}^0, -\overline{C}_T > 0} &= \frac{1}{2} N_{\bar{D}^0}(1 + \overline{A}_T), \\
N_{\bar{D}^0, -\overline{C}_T < 0} &= \frac{1}{2} N_{\bar{D}^0}(1 - \overline{A}_T).
\end{aligned}
\tag{4.1}
$$

The CP-violating asymmetry $a_{CP}^{T\text{-odd}}$ is then calculated from A_T and $\overline{A}_T$. Negligible correlation is found between these two asymmetries. The results of the fit are shown in figure 1. The number of signal decays for each subsample are listed in table 1.

Three different approaches have been followed to search for CPV: a measurement integrated over the phase space, measurements in different regions of phase space, and measurements as a function of the D^0 decay time. The results of the first approach are obtained by fitting the full data sample and are $A_T = (-7.18 \pm 0.41)\%$, and $\overline{A}_T = (-7.55 \pm 0.41)\%$, where the uncertainties are statistical only. The CP-violating asymmetry calculated from the two partial asymmetries is $a_{CP}^{T\text{-odd}} = (0.18 \pm 0.29)\%$.
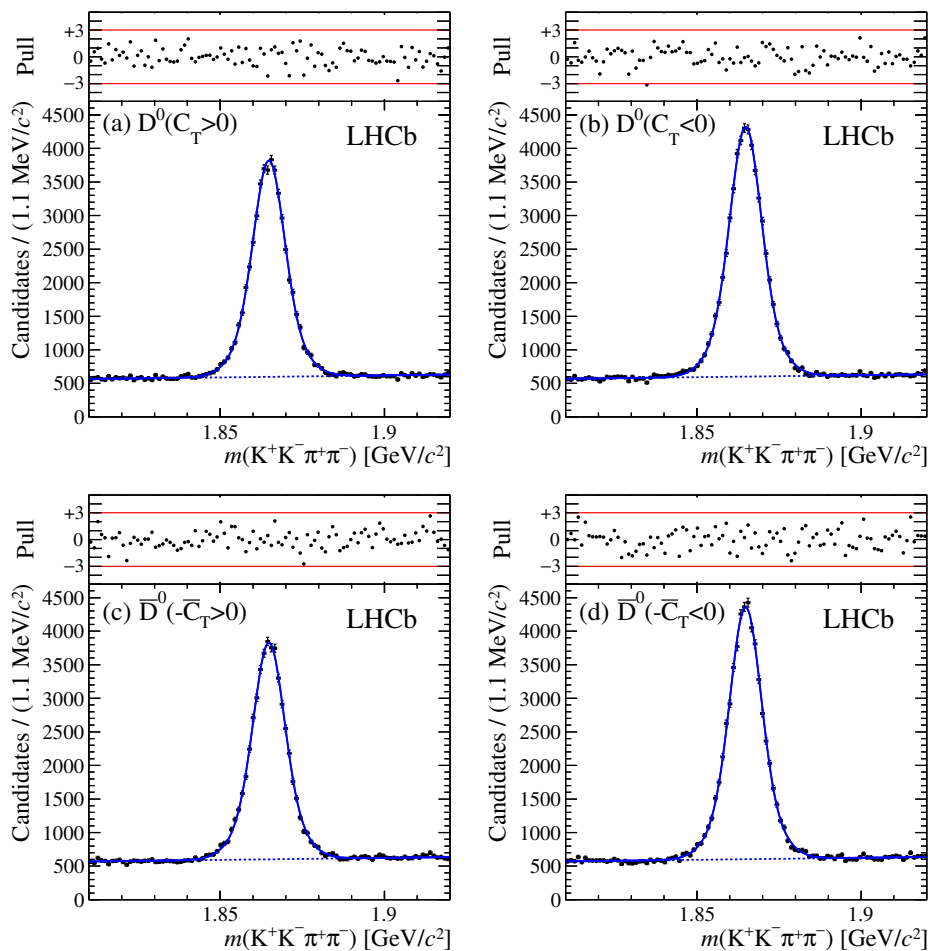
Figure 1. Distributions of the $K^+K^-\pi^+\pi^-$ invariant mass in the four samples defined by D^0 ($\bar{D}^0$) flavour and the sign of C_T ($\overline{C}_T$). The results of the fit are overlaid as a solid line, and a dashed line is used for representing the background. The normalised residuals (pulls) of the difference between the fit results and the data points, divided by their uncertainties, are shown on top of each distribution.

The relatively large asymmetries observed in A_T and $\overline{A}_T$ are due to FSI effects [9, 10], which are known to be relevant in charm mesons decays. These effects are difficult to predict, since they involve non-perturbative strong interactions [27]. However, experimental measurements provide solid anchor points for future calculations.

The measurement in different regions of the phase space is performed by dividing the sample using a binning scheme based on the Cabibbo-Maksimowicz [28] variables $m_{K^+K^-}$, $m_{\pi^+\pi^-}$, $\cos(\theta_{K^+})$, $\cos(\theta_{\pi^+})$, Φ, defined as the K^+K^- and $\pi^+\pi^-$ invariant masses, the cosine of the angle of the K^+ (π^+) with respect to the opposite direction to the D^0 momentum in the K^+K^- ($\pi^+\pi^-$) rest frame, and the angle between the planes described by the two kaons and pions in the D^0 rest frame, respectively.

The background-subtracted distributions for D^0 ($\bar{D}^0$) events with $C_T > 0$ and $C_T < 0$ ($-\overline{C}_T > 0$ and $-\overline{C}_T < 0$) in $m_{\pi^+\pi^-}$ and $m_{K^+K^-}$ are shown in figure 2. The background subtraction is performed using $m(K^+K^-\pi^+\pi^-)$ sidebands. Clear indications of $\rho^0 \to \pi^+\pi^-$
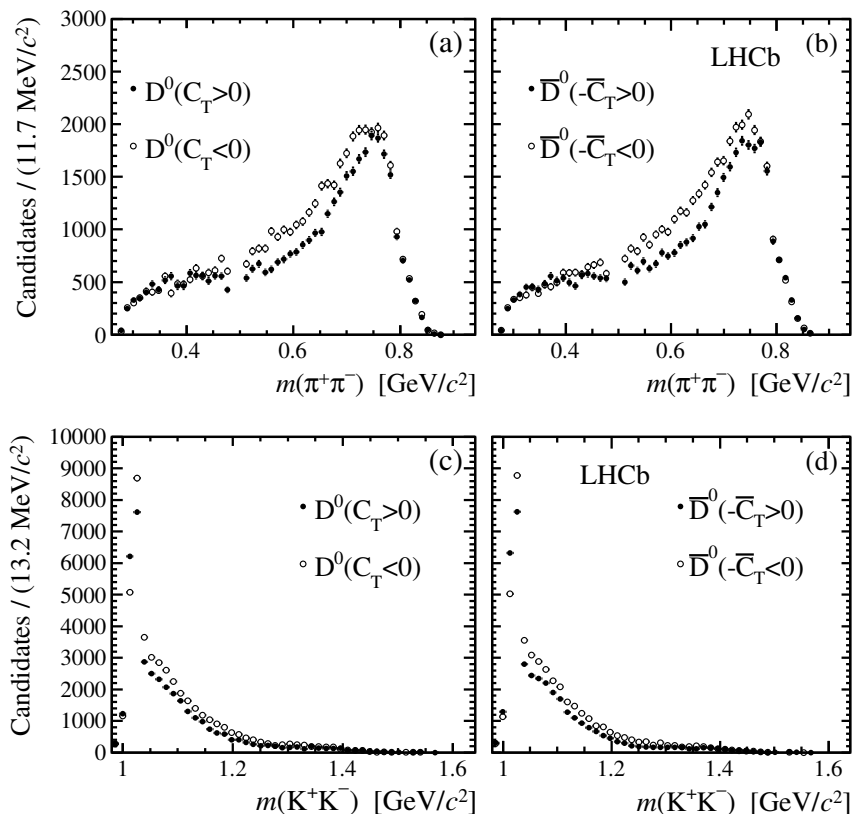
Figure 2. Sideband-subtracted distributions of D^0 ($\bar{D}^0$) candidates in variables of (a, b) $m_{\pi^+\pi^-}$ and (c, d) $m_{K^+K^-}$ for different values of C_T ($\bar{C}_T$). The veto for $D^0 \to K^0_S K^+ K^-$ decays is visible in the $m_{\pi^+\pi^-}$ distribution.

and $\phi \to K^+K^-$ resonances are seen in the data. The distributions of $\cos(\theta_{K^+})$, $\cos(\theta_{\pi^+})$, and Φ variables are shown in figure 3, where FSI-induced differences are clearly evident [29]. Effects of CPV would lead to different distributions for D^0 and $\bar{D}^0$ events.

The phase space is divided in 32 regions such that the number of signal events is similar in each region; the definition of the 32 regions is reported in table 3 in appendix A.

The same fit model used for the integrated measurement is separately fitted to data in each bin. The signal shapes are consistent among different bins, while significant variations are found in the distribution of the combinatorial background. The distributions of the measured asymmetries in the 32-region binning scheme are shown in figure 4 and the results are reported in table 4 in appendix A.

The compatibility with the CP conservation hypothesis is tested by means of a χ^2 test, where the χ^2 is defined as $R^T V^{-1} R$, where R is the array of $a_{CP}^{T\text{-odd}}$ measurements, and V^{-1} is the inverse of the covariance matrix V, defined as the sum of the statistical and systematic covariance matrices. An average systematic uncertainty, whose evaluation is discussed in section 5, is assumed for the different bins. The statistical uncertainties are considered uncorrelated among the bins, while systematic uncertainties are assumed to be fully correlated. The contribution of systematic uncertainties is small compared to the statistical ones, as shown in table 2. The results are consistent with the CP conservation
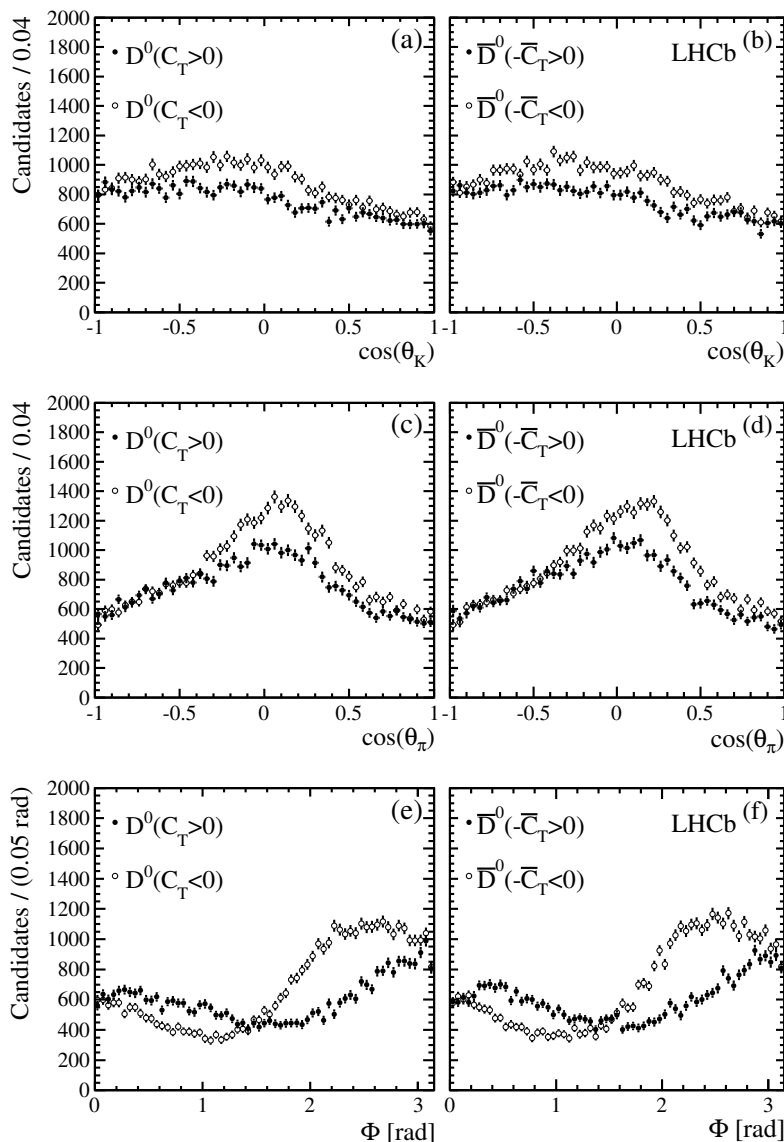
Figure 3. Sideband-subtracted distributions of D^0 ($\bar{D}^0$) candidates in variables of (a, b) $\cos(\theta_{K^+})$, (c, d) $\cos(\theta_{\pi^+})$, and (e, f) Φ for different values of C_T ($\bar{C}_T$). The asymmetric distributions with respect to 0 for $\cos(\theta_{K^+})$ and $\cos(\theta_{\pi^+})$ variables, and with respect to $\pi/2$ for the Φ variable, are due to the dynamics of the four-body decay.

hypothesis with a p-value of 74%, based on $\chi^2/\mathrm{ndf} = 26.4/32$, where ndf is the number of degrees of freedom. Four alternative binning schemes, one with 8 regions and three with 16 regions, are also tested. These are described in appendix A. Results are compatible with the CP conservation hypothesis with a p-value of 24% for the case of 8 regions and 28%, 62%, 82% for the three different phase space divisions in 16 regions. The A_T and $\bar{A}_T$ asymmetries are significantly different among the different regions. This effect can be explained by the rich resonant structure of the hadronic four-body decay [30] that produces different FSI effects over the phase space.

– 7 –
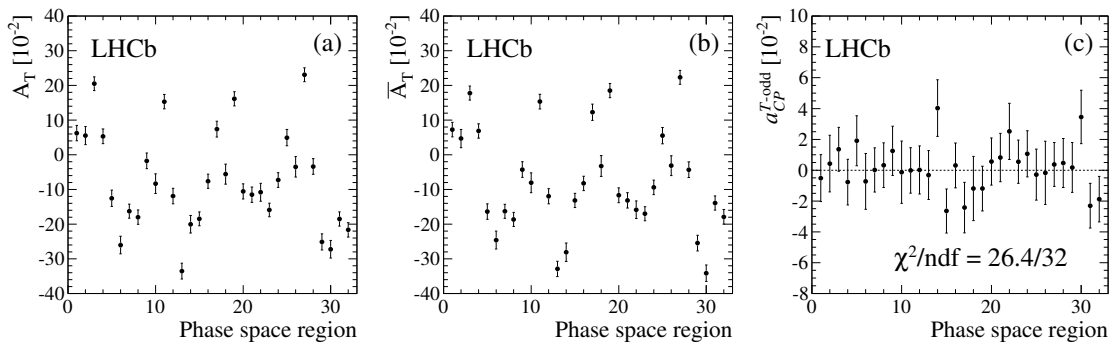
Figure 4. Distributions of the asymmetry parameters (a) A_T, (b) $\overline{A}_T$ and (c) $a_{CP}^{T\text{-odd}}$ in 32 regions of the phase space.
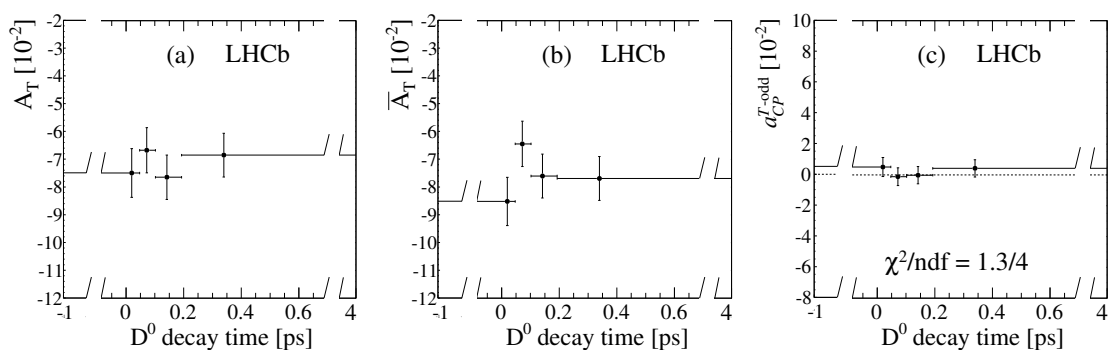
Figure 5. Distributions of the asymmetry parameters (a) A_T, (b) $\overline{A}_T$ and (c) $a_{CP}^{T\text{-odd}}$ as a function of the D^0 decay time. For $a_{CP}^{T\text{-odd}}$, the value of the χ^2/ndf for the CP conservation hypothesis, represented by a dashed line, is also quoted. The scale is broken for the first and last bin.

The $a_{CP}^{T\text{-odd}}$ distribution in D^0 decay time is shown in figure 5 and the results for the different decay time bins are reported in table 5 in appendix B. The compatibility with the CP conservation hypothesis is verified by means of a χ^2 test considering statistical and systematic uncertainties as in the previous case; a value of χ^2/ndf = 1.3/4 is obtained, corresponding to a p-value of 86%. Consistent results are obtained when using different divisions of the decay time in 3 and 5 intervals compatible with the CP conservation hypothesis with p-values of 92% and 83%, respectively. This result is consistent with no time-dependent CPV. The A_T and $\overline{A}_T$ asymmetry parameters do not show any significant dependence as a function of the decay time, and the results are compatible with constant functions with p-values of 80% and 38%, respectively.

5   Systematic uncertainties

The sources of systematic uncertainty and their relative contributions to the total uncertainty are listed in table 2.

The contamination from prompt D^0 decays affects the asymmetry A according to $A \to A(1-f) + fA^d$, where f is the fraction of the contamination in the selected sample

Contribution	$\Delta A_T(\%)$	$\Delta \overline{A}_T(\%)$	$\Delta a_{CP}^{T\text{-odd}}(\%)$
Prompt background	± 0.09	± 0.08	± 0.00
Detector bias	± 0.04	± 0.04	± 0.04
C_T resolution	± 0.02	± 0.03	± 0.01
Fit model	± 0.01	± 0.01	± 0.01
Flavour misidentification	± 0.08	± 0.07	± 0.00
Total	± 0.13	± 0.12	± 0.04

Table 2. Considered sources of systematic uncertainty and their relative contributions to the total uncertainty.

and A^d is its own asymmetry. The uncertainties are evaluated by using as input the fraction f_{prompt} and the asymmetries of the prompt charm sample. These events correspond to random combinations of muons with D^0 originating at the primary vertex and show no significant evidence of correlation between the flavour of the D^0 and the charge of the muon. Assuming that the flavour mistag rate for the prompt D^0 and $\bar{D}^0$ samples is 0.5, these are related to the signal asymmetries as: $A_T^d = a_{CP}^{T\text{-odd}}$, $\overline{A}_T^d = -a_{CP}^{T\text{-odd}}$, and $a_{CP}^{T\text{-odd}d} = a_{CP}^{T\text{-odd}}$.

The detector bias is tested by measuring $a_{CP}^{T\text{-odd}}(D^0 \to K^- \pi^+ \pi^- \pi^+)$ on the $D^0 \to K^- \pi^+ \pi^+ \pi^-$ control sample. In this case, a kinematic selection is required between the pair of pions with identical charge to define the C_T and $\overline{C}_T$ triple products. The pion with higher momentum is used to calculate the triple product. Since this is a Cabibbo-favoured decay, the CP-violating effects are assumed to be negligible, and any significant deviation from zero is considered as a bias introduced by the experimental technique and the detector reconstruction. The asymmetry obtained on the control sample is compatible with no bias, $a_{CP}^{T\text{-odd}}(D^0 \to K^- \pi^+ \pi^- \pi^+) = (0.05 \pm 0.04)\%$. A systematic uncertainty equal to the statistical uncertainty of this measurement is assigned. The test was repeated for different regions of phase space with consistent results.

The systematic uncertainty from detector resolution on C_T is estimated from a simulated sample of $D^0 \to K^+ K^- \pi^+ \pi^-$ decays where neither FSI nor CP-violating effects are present. The difference between the reconstructed and generated asymmetry is considered as a systematic uncertainty due to this effect.

The fit models for signal and background are modified, ensuring good fit quality, to account for model-dependent uncertainties. The signal shape is described with a Gaussian function plus a second Gaussian function with a low-mass power-law tail. The background is described with a third-order polynomial function. Alternative models are fitted to the data and for each model 1000 simulated samples are generated according to fit results. The nominal model is then fitted to the simulated samples and the asymmetry parameters are extracted. Since the bias is not significantly different from zero, its statistical uncertainty is taken as the systematic uncertainty due to this source.

Wrongly identified muon candidates could affect the CP-violating asymmetry as

$$a_{CP}^{T\text{-odd}} \to a_{CP}^{T\text{-odd}} - \Delta\omega/2(A_T + \overline{A}_T), \tag{5.1}$$

where $\Delta\omega \equiv \omega^+ - \omega^-$ is the difference between the probability of assigning a wrong D^0 (ω^+) and $\bar{D}^0$ (ω^-) flavour. Similar considerations enable the estimation of the uncertainty on A_T ($\overline{A}_T$) as $(A_T + \overline{A}_T)\omega^+$ $((A_T + \overline{A}_T)\omega^-)$. The mistag probabilities are measured by reconstructing the double-tagged decay channel $B \to D^{*+}\mu^- X$, with $D^{*+} \to D^0\pi^+$ and $D^0 \to K^+K^-\pi^+\pi^-$, and calculating the fraction of events for which the charge of the muon is identical to the charge of the soft pion from D^{*+} decay. Mistag probabilities of $\omega^+ = (5.2 \pm 1.0) \times 10^{-3}$ and $\omega^- = (4.7 \pm 1.0) \times 10^{-3}$ are measured for D^0 and $\bar{D}^0$ flavour, respectively.

Since the various contributions to the systematic uncertainty are independent, the total uncertainty is obtained by summing them in quadrature, and it is very small. In particular, the $a_{CP}^{T\text{-odd}}$ observable is insensitive to the production asymmetry of D^0 and $\bar{D}^0$ and to reconstruction-induced charge asymmetries. Further cross-checks are made for establishing the stability of the results with respect to the different periods of data taking, different magnet polarities, the choice made in the selection of multiple candidates, and the effect of selection through particle identification criteria. All these tests reported effects compatible to statistical fluctuations, and therefore are not included in the systematic uncertainty.

The total systematic uncertainties reported in table 2 are used for the measurement of the asymmetries in all regions of phase space and in all bins of D^0 decay time.

6 Conclusions

In conclusion, a search for CPV in $D^0 \to K^+K^-\pi^+\pi^-$ decays produced in $B \to D^0\mu^- X$ transitions has been performed. The data sample consists of about 171 300 signal decays. Three different approaches have been followed to exploit the full potential of the data: a measurement integrated over the phase space, measurements in different regions of the phase space, and measurements as a function of the D^0 decay time.

The results from the phase space integrated measurement,

$$A_T = (-7.18 \pm 0.41(\text{stat}) \pm 0.13(\text{syst}))\%,$$
$$\overline{A}_T = (-7.55 \pm 0.41(\text{stat}) \pm 0.12(\text{syst}))\%,$$
$$a_{CP}^{T\text{-odd}} = (0.18 \pm 0.29(\text{stat}) \pm 0.04(\text{syst}))\%,$$

are consistent with those measured in ref. [12], with significantly improved statistical and systematic uncertainties. The evaluation of the systematic uncertainties is based mostly on high statistics control samples.

An analysis of the asymmetries in different regions of the phase space is made for the first time and the results are consistent with CP conservation. Relatively large variations of A_T and $\overline{A}_T$ over the phase space are measured, which are due to FSI effects produced in the rich resonant structure of the decay [29, 30]. For the first time the $a_{CP}^{T\text{-odd}}$ asymmetry is measured as a function of the D^0 decay time and does not show any significant structure at the observed sensitivity. These results further constrain extensions of the SM [2].

Region	Φ	$m_{\pi^+\pi^-}$ (GeV/c^2)	$m_{K^+K^-}$ (GeV/c^2)	$\cos(\theta_{\pi^+})$	$\cos(\theta_{K^+})$
1	(0.00, 1.99)	(0.20, 0.65)	(0.60, 1.08)	(−1.00, −0.22)	(−1.00, −0.28)
2	(0.00, 1.99)	(0.20, 0.65)	(1.08, 1.70)	(−1.00, −0.24)	(−1.00, −0.14)
3	(0.00, 1.99)	(0.65, 1.00)	(0.60, 1.02)	(−1.00, −0.09)	(−1.00, −0.03)
4	(0.00, 1.99)	(0.65, 1.00)	(1.02, 1.70)	(−1.00, −0.09)	(−1.00, −0.26)
5	(1.99, 3.14)	(0.20, 0.68)	(0.60, 1.12)	(−1.00, −0.02)	(−1.00, −0.04)
6	(1.99, 3.14)	(0.20, 0.68)	(1.12, 1.70)	(−1.00, 0.01)	(−1.00, 0.07)
7	(1.99, 3.14)	(0.68, 1.00)	(0.60, 1.04)	(−1.00, 0.28)	(−1.00, −0.05)
8	(1.99, 3.14)	(0.68, 1.00)	(1.04, 1.70)	(−1.00, 0.27)	(−1.00, −0.08)
9	(0.00, 1.99)	(0.20, 0.65)	(0.60, 1.08)	(−0.22, 1.00)	(−1.00, −0.28)
10	(0.00, 1.99)	(0.20, 0.65)	(1.08, 1.70)	(−0.24, 1.00)	(−1.00, −0.15)
11	(0.00, 1.99)	(0.65, 1.00)	(0.60, 1.02)	(−0.09, 1.00)	(−1.00, −0.03)
12	(1.99, 3.14)	(0.20, 0.68)	(0.60, 1.12)	(−0.02, 1.00)	(−1.00, −0.04)
13	(1.99, 3.14)	(0.20, 0.68)	(1.12, 1.70)	(0.01, 1.00)	(−1.00, 0.07)
14	(1.99, 3.14)	(0.68, 1.00)	(0.60, 1.04)	(0.28, 1.00)	(−1.00, −0.05)
15	(1.99, 3.14)	(0.68, 1.00)	(1.04, 1.70)	(0.27, 1.00)	(−1.00, −0.08)
16	(0.00, 1.99)	(0.20, 0.65)	(0.60, 1.08)	(−1.00, 0.10)	(−0.28, 1.00)
17	(0.00, 1.99)	(0.20, 0.65)	(1.08, 1.70)	(−1.00, 0.01)	(−0.15, 1.00)
18	(0.00, 1.99)	(0.65, 1.00)	(0.60, 1.02)	(−1.00, 0.28)	(−0.03, 1.00)
19	(0.00, 1.99)	(0.65, 1.00)	(1.02, 1.70)	(−1.00, −0.12)	(−0.26, 1.00)
20	(1.99, 3.14)	(0.20, 0.68)	(0.60, 1.12)	(−1.00, 0.07)	(−0.04, 1.00)
21	(1.99, 3.14)	(0.20, 0.68)	(1.12, 1.70)	(−1.00, 0.11)	(0.07, 1.00)
22	(1.99, 3.14)	(0.68, 1.00)	(0.60, 1.04)	(−1.00, −0.13)	(−0.05, 1.00)
23	(1.99, 3.14)	(0.68, 1.00)	(1.04, 1.70)	(−1.00, −0.15)	(−0.08, 1.00)
24	(0.00, 1.99)	(0.20, 0.65)	(0.60, 1.08)	(0.10, 1.00)	(−0.28, 1.00)
25	(0.00, 1.99)	(0.20, 0.65)	(1.08, 1.70)	(0.01, 1.00)	(−0.15, 1.00)
26	(0.00, 1.99)	(0.65, 1.00)	(0.60, 1.02)	(0.28, 1.00)	(−0.03, 1.00)
27	(0.00, 1.99)	(0.65, 1.00)	(1.02, 1.70)	(−0.12, 1.00)	(−0.26, 1.00)
28	(1.99, 3.14)	(0.20, 0.68)	(0.60, 1.12)	(0.07, 1.00)	(−0.04, 1.00)
29	(1.99, 3.14)	(0.20, 0.68)	(1.12, 1.70)	(0.11, 1.00)	(0.07, 1.00)
30	(1.99, 3.14)	(0.68, 1.00)	(0.60, 1.04)	(−0.13, 1.00)	(−0.05, 1.00)
31	(0.00, 1.99)	(0.65, 1.00)	(1.02, 1.70)	(−0.10, 1.00)	(−1.00, −0.26)
32	(1.99, 3.14)	(0.68, 1.00)	(1.04, 1.70)	(−0.15, 1.00)	(−0.08, 1.00)

Table 3. Definition of the 32 regions of the five-dimensional phase space of the four-body $D^0 \to K^+ K^- \pi^+ \pi^-$ decay.

A Measured asymmetries in regions of phase space

The definitions of the 32 regions of phase space of the four-body $D^0 \to K^+ K^- \pi^+ \pi^-$ decay are reported in table 3. The measurements in each region of phase space for the $a_{CP}^{T\text{-odd}}$, A_T, and $\overline{A}_T$ are reported in table 4.

The alternative binning schemes with 8 and 16 bins have been defined by integrating over $\cos(\theta_{K^+})$ and $\cos(\theta_{\pi^+})$ (8 bins), $\cos(\theta_{K^+})$ (16 bins), $\cos(\theta_{\pi^+})$ (16 bins), and by using mass variables ($m_{K^-\pi^+}$, $m_{K^+K^-\pi^+}$, $m_{K^-\pi^+\pi^-}$) in place of the angular variables (16 bins).

		Region 1	Region 2	Region 3	Region 4	Region 5
$a_{CP}^{T\text{-odd}}$	(%)	-0.51 ± 1.53	0.43 ± 1.84	1.36 ± 1.42	-0.77 ± 1.48	1.91 ± 1.62
A_T	(%)	6.25 ± 2.21	5.54 ± 2.59	20.51 ± 1.98	5.33 ± 2.10	-12.54 ± 2.37
$\overline{A}_T$	(%)	7.28 ± 2.10	4.68 ± 2.61	17.79 ± 2.04	6.87 ± 2.09	-16.37 ± 2.22
		Region 6	Region 7	Region 8	Region 9	Region 10
$a_{CP}^{T\text{-odd}}$	(%)	-0.73 ± 1.81	0.01 ± 1.43	0.32 ± 1.45	1.26 ± 1.60	-0.13 ± 2.02
A_T	(%)	-26.04 ± 2.54	-16.27 ± 2.03	-17.99 ± 2.06	-1.74 ± 2.27	-8.32 ± 2.86
$\overline{A}_T$	(%)	-24.59 ± 2.58	-16.30 ± 2.03	-18.63 ± 2.04	-4.25 ± 2.25	-8.06 ± 2.86
		Region 11	Region 12	Region 13	Region 14	Region 15
$a_{CP}^{T\text{-odd}}$	(%)	-0.01 ± 1.48	0.02 ± 1.56	-0.32 ± 1.59	4.03 ± 1.84	-2.64 ± 1.43
A_T	(%)	15.32 ± 2.07	-11.92 ± 2.24	-33.55 ± 2.26	-20.03 ± 2.55	-18.45 ± 2.00
$\overline{A}_T$	(%)	15.35 ± 2.11	-11.96 ± 2.18	-32.91 ± 2.22	-28.09 ± 2.64	-13.17 ± 2.04
		Region 16	Region 17	Region 18	Region 19	Region 20
$a_{CP}^{T\text{-odd}}$	(%)	0.31 ± 1.45	-2.43 ± 1.64	-1.18 ± 2.08	-1.19 ± 1.45	0.56 ± 1.53
A_T	(%)	-7.63 ± 2.06	7.42 ± 2.28	-5.60 ± 2.89	16.15 ± 2.05	-10.57 ± 2.19
$\overline{A}_T$	(%)	-8.25 ± 2.05	12.28 ± 2.35	-3.23 ± 3.00	18.53 ± 2.04	-11.69 ± 2.15
		Region 21	Region 22	Region 23	Region 24	Region 25
$a_{CP}^{T\text{-odd}}$	(%)	0.82 ± 1.57	2.52 ± 1.82	0.55 ± 1.41	1.06 ± 1.49	-0.29 ± 1.66
A_T	(%)	-11.50 ± 2.22	-10.81 ± 2.59	-15.90 ± 1.96	-7.27 ± 2.11	4.95 ± 2.34
$\overline{A}_T$	(%)	-13.15 ± 2.21	-15.85 ± 2.55	-17.00 ± 2.02	-9.40 ± 2.11	5.53 ± 2.34
		Region 26	Region 27	Region 28	Region 29	Region 30
$a_{CP}^{T\text{-odd}}$	(%)	-0.17 ± 2.05	0.37 ± 1.42	0.46 ± 1.59	0.18 ± 1.62	3.45 ± 1.73
A_T	(%)	-3.47 ± 2.94	23.09 ± 2.01	-3.37 ± 2.26	-25.11 ± 2.32	-27.24 ± 2.53
$\overline{A}_T$	(%)	-3.13 ± 2.87	22.34 ± 2.02	-4.30 ± 2.25	-25.47 ± 2.25	-34.15 ± 2.36
		Region 31	Region 32			
$a_{CP}^{T\text{-odd}}$	(%)	-2.30 ± 1.45	-1.88 ± 1.47			
A_T	(%)	-18.51 ± 2.06	-21.65 ± 2.05			
$\overline{A}_T$	(%)	-13.91 ± 2.04	-17.89 ± 2.12			

Table 4. Measurements of $a_{CP}^{T\text{-odd}}$, A_T and $\overline{A}_T$ in each region of phase space. The uncertainties are statistical only. A common systematic uncertainty of 0.13%, 0.12% and 0.04% should be added to the asymmetries A_T, $\overline{A}_T$ and $a_{CP}^{T\text{-odd}}$, respectively. This uncertainty is considered fully correlated among the bins.

	[−1.00, 0.05]	[0.05, 0.10]	[0.10, 0.19]	[0.19, 4.00]
$a_{CP}^{T\text{-odd}}$ (%)	0.51 ± 0.62	-0.12 ± 0.58	-0.02 ± 0.56	0.42 ± 0.56
A_T (%)	-7.49 ± 0.88	-6.67 ± 0.81	-7.64 ± 0.80	-6.84 ± 0.79
$\overline{A}_T$ (%)	-8.51 ± 0.87	-6.44 ± 0.82	-7.60 ± 0.79	-7.68 ± 0.79

Table 5. Measurements of $a_{CP}^{T\text{-odd}}$, A_T and $\overline{A}_T$ in different intervals of D^0 decay time, t, expressed in ps. The uncertainties are statistical only. A common systematic uncertainty of 0.13%, 0.12% and 0.04% should be added to the asymmetries A_T, $\overline{A}_T$ and $a_{CP}^{T\text{-odd}}$, respectively. This uncertainty is considered fully correlated among the bins.

B   Measured asymmetries in intervals of D^0 decay time

The values measured in 4 different intervals of the D^0 decay time for $a_{CP}^{T\text{-odd}}$, A_T, and $\overline{A}_T$ are reported in table 5.

References

[1] S. Bianco, F.L. Fabbri, D. Benson and I. Bigi, *A Cicerone for the physics of charm*, *Riv. Nuovo Cim.* **26N7** (2003) 1 [hep-ex/0309021] [INSPIRE].

[2] Y. Grossman, A.L. Kagan and Y. Nir, *New physics and CP-violation in singly Cabibbo suppressed D decays*, *Phys. Rev.* **D 75** (2007) 036008 [hep-ph/0609178] [INSPIRE].

[3] T. Feldmann, S. Nandi and A. Soni, *Repercussions of flavour symmetry breaking on CP-violation in D-meson decays*, *JHEP* **06** (2012) 007 [arXiv:1202.3795] [INSPIRE].

[4] J. Brod, A.L. Kagan and J. Zupan, *Size of direct CP-violation in singly Cabibbo-suppressed D decays*, *Phys. Rev.* **D 86** (2012) 014023 [arXiv:1111.5000] [INSPIRE].

[5] B. Bhattacharya, M. Gronau and J.L. Rosner, *CP asymmetries in singly-Cabibbo-suppressed D decays to two pseudoscalar mesons*, *Phys. Rev.* **D 85** (2012) 054014 [arXiv:1201.2351] [INSPIRE].

[6] LHCb collaboration, *Model-independent search for CP violation in $D^0 \to K^- K^+ \pi^- \pi^+$ and $D^0 \to \pi^- \pi^+ \pi^+ \pi^-$ decays*, *Phys. Lett.* **B 726** (2013) 623 [arXiv:1308.3189] [INSPIRE].

[7] G. Valencia, *Angular correlations in the decay $B \to VV$ and CP violation*, *Phys. Rev.* **D 39** (1989) 3339 [INSPIRE].

[8] A. Datta and D. London, *Triple-product correlations in $B \to V_1 V_2$ decays and new physics*, *Int. J. Mod. Phys.* **A 19** (2004) 2505 [hep-ph/0303159] [INSPIRE].

[9] I.I.Y. Bigi, *Charm physics: like Botticelli in the Sistine Chapel*, hep-ph/0107102 [INSPIRE].

[10] M. Gronau and J.L. Rosner, *Triple product asymmetries in K, $D_{(s)}$ and $B_{(s)}$ decays*, *Phys. Rev.* **D 84** (2011) 096013 [arXiv:1107.1232] [INSPIRE].

[11] FOCUS collaboration, J.M. Link et al., *Search for T violation in charm meson decays*, *Phys. Lett.* **B 622** (2005) 239 [hep-ex/0506012] [INSPIRE].

[12] BaBar collaboration, P. del Amo Sanchez et al., *Search for CP-violation using T-odd correlations in $D^0 \to K^+ K^- \pi^+ \pi^-$ decays*, *Phys. Rev.* **D 81** (2010) 111103 [arXiv:1003.3397] [INSPIRE].

[13] LHCb collaboration, *The LHCb detector at the LHC*, 2008 *JINST* **3** S08005 [INSPIRE].

[14] R. Aaij et al., *Performance of the LHCb Vertex Locator*, 2014 *JINST* **9** P09007 [arXiv:1405.7808] [INSPIRE].

[15] LHCb OUTER TRACKER GROUP collaboration, *Performance of the LHCb Outer Tracker*, 2014 *JINST* **9** P01002 [arXiv:1311.3893] [INSPIRE].

[16] LHCb RICH GROUP collaboration, *Performance of the LHCb RICH detector at the LHC*, *Eur. Phys. J.* **C 73** (2013) 2431 [arXiv:1211.6759] [INSPIRE].

[17] A.A. Alves Jr. et al., *Performance of the LHCb muon system*, 2013 *JINST* **8** P02022 [arXiv:1211.1346] [INSPIRE].

[18] R. Aaij et al., *The LHCb Trigger and its Performance in 2011*, 2013 *JINST* **8** P04022 [arXiv:1211.3055] [INSPIRE].

[19] T. Sjöstrand, S. Mrenna and P.Z. Skands, *PYTHIA 6.4 Physics and Manual*, *JHEP* **05** (2006) 026 [hep-ph/0603175] [INSPIRE].

[20] T. Sjöstrand, S. Mrenna and P.Z. Skands, *A brief introduction to PYTHIA 8.1*, *Comput. Phys. Commun.* **178** (2008) 852 [arXiv:0710.3820] [INSPIRE].

[21] I. Belyaev et al., *Handling of the generation of primary events in Gauss, the LHCb simulation framework*, *IEEE Nucl. Sci. Symp. Conf. Rec.* **2010** (2010) 1155.

[22] D.J. Lange, *The EvtGen particle decay simulation package*, *Nucl. Instrum. Meth.* **A 462** (2001) 152 [INSPIRE].

[23] GEANT4 collaboration, J. Allison et al., *GEANT4: developments and applications*, *IEEE Trans. Nucl. Sci.* **53** (2006) 270.

[24] GEANT4 collaboration, S. Agostinelli et al., *GEANT4: a simulation toolkit*, *Nucl. Instrum. Meth.* **A 506** (2003) 250 [INSPIRE].

[25] M. Clemencic et al., *The LHCb simulation application, Gauss: design, evolution and experience*, *J. Phys. Conf. Ser.* **331** (2011) 032023 [INSPIRE].

[26] PARTICLE DATA GROUP collaboration, J. Beringer et al., *Review of Particle Physics (RPP)*, *Phys. Rev.* **D 86** (2012) 010001 [INSPIRE].

[27] M. Gronau, *Resonant two-body D decays*, *Phys. Rev. Lett.* **83** (1999) 4005 [hep-ph/9908237] [INSPIRE].

[28] N. Cabibbo and A. Maksymowicz, *Angular correlations in Ke-4 decays and determination of low-energy $\pi - \pi$ phase shifts*, *Phys. Rev.* **137** (1965) B438.

[29] J.F. Donoghue, *Is $D^0 \to \varphi \overline{K}^0$ really a clear signal for the annihilation diagram?*, *Phys. Rev.* **D 33** (1986) 1516 [INSPIRE].

[30] CLEO collaboration, M. Artuso et al., *Amplitude analysis of $D^0 \to K^+ K^- \pi^+ \pi^-$*, *Phys. Rev.* **D 85** (2012) 122002 [arXiv:1201.5716] [INSPIRE].

The LHCb collaboration

R. Aaij[41], B. Adeva[37], M. Adinolfi[46], A. Affolder[52], Z. Ajaltouni[5], S. Akar[6], J. Albrecht[9],
F. Alessio[38], M. Alexander[51], S. Ali[41], G. Alkhazov[30], P. Alvarez Cartelle[37], A.A. Alves Jr[25,38],
S. Amato[2], S. Amerio[22], Y. Amhis[7], L. An[3], L. Anderlini[17,g], J. Anderson[40], R. Andreassen[57],
M. Andreotti[16,f], J.E. Andrews[58], R.B. Appleby[54], O. Aquines Gutierrez[10], F. Archilli[38],
A. Artamonov[35], M. Artuso[59], E. Aslanides[6], G. Auriemma[25,n], M. Baalouch[5], S. Bachmann[11],
J.J. Back[48], A. Badalov[36], W. Baldini[16], R.J. Barlow[54], C. Barschel[38], S. Barsuk[7], W. Barter[47],
V. Batozskaya[28], V. Battista[39], A. Bay[39], L. Beaucourt[4], J. Beddow[51], F. Bedeschi[23], I. Bediaga[1],
S. Belogurov[31], K. Belous[35], I. Belyaev[31], E. Ben-Haim[8], G. Bencivenni[18], S. Benson[38],
J. Benton[46], A. Berezhnoy[32], R. Bernet[40], M.-O. Bettler[47], M. van Beuzekom[41], A. Bien[11],
S. Bifani[45], T. Bird[54], A. Bizzeti[17,i], P.M. Bjørnstad[54], T. Blake[48], F. Blanc[39], J. Blouw[10],
S. Blusk[59], V. Bocci[25], A. Bondar[34], N. Bondar[30,38], W. Bonivento[15,38], S. Borghi[54], A. Borgia[59],
M. Borsato[7], T.J.V. Bowcock[52], E. Bowen[40], C. Bozzi[16], T. Brambach[9], J. Bressieux[39], D. Brett[54],
M. Britsch[10], T. Britton[59], J. Brodzicka[54], N.H. Brook[46], H. Brown[52], A. Bursche[40], G. Busetto[22,r],
J. Buytaert[38], S. Cadeddu[15], R. Calabrese[16,f], M. Calvi[20,k], M. Calvo Gomez[36,p], P. Campana[18,38],
D. Campora Perez[38], A. Carbone[14,d], G. Carboni[24,l], R. Cardinale[19,38,j], A. Cardini[15], L. Carson[50],
K. Carvalho Akiba[2], G. Casse[52], L. Cassina[20], L. Castillo Garcia[38], M. Cattaneo[38], Ch. Cauet[9],
R. Cenci[58], M. Charles[8], Ph. Charpentier[38], M. Chefdeville[4], S. Chen[54], S.-F. Cheung[55],
N. Chiapolini[40], M. Chrzaszcz[40,26], K. Ciba[38], X. Cid Vidal[38], G. Ciezarek[53], P.E.L. Clarke[50],
M. Clemencic[38], H.V. Cliff[47], J. Closier[38], V. Coco[38], J. Cogan[6], E. Cogneras[5], L. Cojocariu[29],
P. Collins[38], A. Comerma-Montells[11], A. Contu[15], A. Cook[46], M. Coombes[46], S. Coquereau[8],
G. Corti[38], M. Corvo[16,f], I. Counts[56], B. Couturier[38], G.A. Cowan[50], D.C. Craik[48],
M. Cruz Torres[60], S. Cunliffe[53], R. Currie[50], C. D'Ambrosio[38], J. Dalseno[46], P. David[8],
P.N.Y. David[41], A. Davis[57], K. De Bruyn[41], S. De Capua[54], M. De Cian[11], J.M. De Miranda[1],
L. De Paula[2], W. De Silva[57], P. De Simone[18], D. Decamp[4], M. Deckenhoff[9], L. Del Buono[8],
N. Déléage[4], D. Derkach[55], O. Deschamps[5], F. Dettori[38], A. Di Canto[38], H. Dijkstra[38],
S. Donleavy[52], F. Dordei[11], M. Dorigo[39], A. Dosil Suárez[37], D. Dossett[48], A. Dovbnya[43],
K. Dreimanis[52], G. Dujany[54], F. Dupertuis[39], P. Durante[38], R. Dzhelyadin[35], A. Dziurda[26],
A. Dzyuba[30], S. Easo[49,38], U. Egede[53], V. Egorychev[31], S. Eidelman[34], S. Eisenhardt[50],
U. Eitschberger[9], R. Ekelhof[9], L. Eklund[51], I. El Rifai[5], Ch. Elsasser[40], S. Ely[59], S. Esen[11],
H.-M. Evans[47], T. Evans[55], A. Falabella[14], C. Färber[11], C. Farinelli[41], N. Farley[45], S. Farry[52],
RF Fay[52], D. Ferguson[50], V. Fernandez Albor[37], F. Ferreira Rodrigues[1], M. Ferro-Luzzi[38],
S. Filippov[33], M. Fiore[16,f], M. Fiorini[16,f], M. Firlej[27], C. Fitzpatrick[39], T. Fiutowski[27], P. Fol[53],
M. Fontana[10], F. Fontanelli[19,j], R. Forty[38], O. Francisco[2], M. Frank[38], C. Frei[38], M. Frosini[17,38,g],
J. Fu[21,38], E. Furfaro[24,l], A. Gallas Torreira[37], D. Galli[14,d], S. Gallorini[22], S. Gambetta[19,j],
M. Gandelman[2], P. Gandini[59], Y. Gao[3], J. García Pardiñas[37], J. Garofoli[59], J. Garra Tico[47],
L. Garrido[36], C. Gaspar[38], R. Gauld[55], L. Gavardi[9], G. Gavrilov[30], A. Geraci[21,v], E. Gersabeck[11],
M. Gersabeck[54], T. Gershon[48], Ph. Ghez[4], A. Gianelle[22], S. Gianì[39], V. Gibson[47], L. Giubega[29],
V.V. Gligorov[38], C. Göbel[60], D. Golubkov[31], A. Golutvin[53,31,38], A. Gomes[1,a], C. Gotti[20],
M. Grabalosa Gándara[5], R. Graciani Diaz[36], L.A. Granado Cardoso[38], E. Graugés[36], G. Graziani[17],
A. Grecu[29], E. Greening[55], S. Gregson[47], P. Griffith[45], L. Grillo[11], O. Grünberg[62], B. Gui[59],
E. Gushchin[33], Yu. Guz[35,38], T. Gys[38], C. Hadjivasiliou[59], G. Haefeli[39], C. Haen[38], S.C. Haines[47],
S. Hall[53], B. Hamilton[58], T. Hampson[46], X. Han[11], S. Hansmann-Menzemer[11], N. Harnew[55],
S.T. Harnew[46], J. Harrison[54], J. He[38], T. Head[38], V. Heijne[41], K. Hennessy[52], P. Henrard[5],
L. Henry[8], J.A. Hernando Morata[37], E. van Herwijnen[38], M. Heß[62], A. Hicheur[1], D. Hill[55],
M. Hoballah[5], C. Hombach[54], W. Hulsbergen[41], P. Hunt[55], N. Hussain[55], D. Hutchcroft[52],
D. Hynds[51], M. Idzik[27], P. Ilten[56], R. Jacobsson[38], A. Jaeger[11], J. Jalocha[55], E. Jans[41], P. Jaton[39],

A. Jawahery[58], F. Jing[3], M. John[55], D. Johnson[55], C.R. Jones[47], C. Joram[38], B. Jost[38], N. Jurik[59],
M. Kaballo[9], S. Kandybei[43], W. Kanso[6], M. Karacson[38], T.M. Karbach[38], S. Karodia[51],
M. Kelsey[59], I.R. Kenyon[45], T. Ketel[42], B. Khanji[20], C. Khurewathanakul[39], S. Klaver[54],
K. Klimaszewski[28], O. Kochebina[7], M. Kolpin[11], I. Komarov[39], R.F. Koopman[42],
P. Koppenburg[41,38], M. Korolev[32], A. Kozlinskiy[41], L. Kravchuk[33], K. Kreplin[11], M. Kreps[48],
G. Krocker[11], P. Krokovny[34], F. Kruse[9], W. Kucewicz[26,o], M. Kucharczyk[20,26,38,k],
V. Kudryavtsev[34], K. Kurek[28], T. Kvaratskheliya[31], V.N. La Thi[39], D. Lacarrere[38], G. Lafferty[54],
A. Lai[15], D. Lambert[50], R.W. Lambert[42], G. Lanfranchi[18], C. Langenbruch[48], B. Langhans[38],
T. Latham[48], C. Lazzeroni[45], R. Le Gac[6], J. van Leerdam[41], J.-P. Lees[4], R. Lefèvre[5], A. Leflat[32],
J. Lefrançois[7], S. Leo[23], O. Leroy[6], T. Lesiak[26], B. Leverington[11], Y. Li[3], T. Likhomanenko[63],
M. Liles[52], R. Lindner[38], C. Linn[38], F. Lionetto[40], B. Liu[15], S. Lohn[38], I. Longstaff[51], J.H. Lopes[2],
N. Lopez-March[39], P. Lowdon[40], H. Lu[3], D. Lucchesi[22,r], H. Luo[50], A. Lupato[22], E. Luppi[16,f],
O. Lupton[55], F. Machefert[7], I.V. Machikhiliyan[31], F. Maciuc[29], O. Maev[30], S. Malde[55],
A. Malinin[63], G. Manca[15,e], G. Mancinelli[6], A. Mapelli[38], J. Maratas[5], J.F. Marchand[4],
U. Marconi[14], C. Marin Benito[36], P. Marino[23,t], R. Märki[39], J. Marks[11], G. Martellotti[25],
A. Martens[8], A. Martín Sánchez[7], M. Martinelli[39], D. Martinez Santos[42], F. Martinez Vidal[64],
D. Martins Tostes[2], A. Massafferri[1], R. Matev[38], Z. Mathe[38], C. Matteuzzi[20], A. Mazurov[45],
M. McCann[53], J. McCarthy[45], A. McNab[54], R. McNulty[12], B. McSkelly[52], B. Meadows[57],
F. Meier[9], M. Meissner[11], M. Merk[41], D.A. Milanes[8], M.-N. Minard[4], N. Moggi[14],
J. Molina Rodriguez[60], S. Monteil[5], M. Morandin[22], P. Morawski[27], A. Mordà[6], M.J. Morello[23,t],
J. Moron[27], A.-B. Morris[50], R. Mountain[59], F. Muheim[50], K. Müller[40], M. Mussini[14], B. Muster[39],
P. Naik[46], T. Nakada[39], R. Nandakumar[49], I. Nasteva[2], M. Needham[50], N. Neri[21], S. Neubert[38],
N. Neufeld[38], M. Neuner[11], A.D. Nguyen[39], T.D. Nguyen[39], C. Nguyen-Mau[39,q], M. Nicol[7],
V. Niess[5], R. Niet[9], N. Nikitin[32], T. Nikodem[11], A. Novoselov[35], D.P. O'Hanlon[48],
A. Oblakowska-Mucha[27], V. Obraztsov[35], S. Oggero[41], S. Ogilvy[51], O. Okhrimenko[44],
R. Oldeman[15,e], G. Onderwater[65], M. Orlandea[29], J.M. Otalora Goicochea[2], P. Owen[53],
A. Oyanguren[64], B.K. Pal[59], A. Palano[13,c], F. Palombo[21,u], M. Palutan[18], J. Panman[38],
A. Papanestis[49,38], M. Pappagallo[51], L.L. Pappalardo[16,f], C. Parkes[54], C.J. Parkinson[9,45],
G. Passaleva[17], G.D. Patel[52], M. Patel[53], C. Patrignani[19,j], A. Pazos Alvarez[37], A. Pearce[54],
A. Pellegrino[41], M. Pepe Altarelli[38], S. Perazzini[14,d], E. Perez Trigo[37], P. Perret[5],
M. Perrin-Terrin[6], L. Pescatore[45], E. Pesen[66], K. Petridis[53], A. Petrolini[19,j], E. Picatoste Olloqui[36],
B. Pietrzyk[4], T. Pilař[48], D. Pinci[25], A. Pistone[19], S. Playfer[50], M. Plo Casasus[37], F. Polci[8],
A. Poluektov[48,34], E. Polycarpo[2], A. Popov[35], D. Popov[10], B. Popovici[29], C. Potterat[2], E. Price[46],
J.D. Price[52], J. Prisciandaro[39], A. Pritchard[52], C. Prouve[46], V. Pugatch[44], A. Puig Navarro[39],
G. Punzi[23,s], W. Qian[4], B. Rachwal[26], J.H. Rademacker[46], B. Rakotomiaramanana[39], M. Rama[18],
M.S. Rangel[2], I. Raniuk[43], N. Rauschmayr[38], G. Raven[42], F. Redi[53], S. Reichert[54], M.M. Reid[48],
A.C. dos Reis[1], S. Ricciardi[49], S. Richards[46], M. Rihl[38], K. Rinnert[52], V. Rives Molina[36],
P. Robbe[7], A.B. Rodrigues[1], E. Rodrigues[54], P. Rodriguez Perez[54], S. Roiser[38], V. Romanovsky[35],
A. Romero Vidal[37], M. Rotondo[22], J. Rouvinet[39], T. Ruf[38], H. Ruiz[36], P. Ruiz Valls[64],
J.J. Saborido Silva[37], N. Sagidova[30], P. Sail[51], B. Saitta[15,e], V. Salustino Guimaraes[2],
C. Sanchez Mayordomo[64], B. Sanmartin Sedes[37], R. Santacesaria[25], C. Santamarina Rios[37],
E. Santovetti[24,l], A. Sarti[18,m], C. Satriano[25,n], A. Satta[24], D.M. Saunders[46], M. Savrie[16,f],
D. Savrina[31,32], M. Schiller[42], H. Schindler[38], M. Schlupp[9], M. Schmelling[10], B. Schmidt[38],
O. Schneider[39], A. Schopper[38], M.-H. Schune[7], R. Schwemmer[38], B. Sciascia[18], A. Sciubba[25],
M. Seco[37], A. Semennikov[31], I. Sepp[53], N. Serra[40], J. Serrano[6], L. Sestini[22], P. Seyfert[11],
M. Shapkin[35], I. Shapoval[16,43,f], Y. Shcheglov[30], T. Shears[52], L. Shekhtman[34], V. Shevchenko[63],
A. Shires[9], R. Silva Coutinho[48], G. Simi[22], M. Sirendi[47], N. Skidmore[46], T. Skwarnicki[59],
N.A. Smith[52], E. Smith[55,49], E. Smith[53], J. Smith[47], M. Smith[54], H. Snoek[41], M.D. Sokoloff[57],

F.J.P. Soler[51], F. Soomro[39], D. Souza[46], B. Souza De Paula[2], B. Spaan[9], A. Sparkes[50], P. Spradlin[51], S. Sridharan[38], F. Stagni[38], M. Stahl[11], S. Stahl[11], O. Steinkamp[40], O. Stenyakin[35], S. Stevenson[55], S. Stoica[29], S. Stone[59], B. Storaci[40], S. Stracka[23,38], M. Straticiuc[29], U. Straumann[40], R. Stroili[22], V.K. Subbiah[38], L. Sun[57], W. Sutcliffe[53], K. Swientek[27], S. Swientek[9], V. Syropoulos[42], M. Szczekowski[28], P. Szczypka[39,38], D. Szilard[2], T. Szumlak[27], S. T'Jampens[4], M. Teklishyn[7], G. Tellarini[16,f], F. Teubert[38], C. Thomas[55], E. Thomas[38], J. van Tilburg[41], V. Tisserand[4], M. Tobin[39], S. Tolk[42], L. Tomassetti[16,f], D. Tonelli[38], S. Topp-Joergensen[55], N. Torr[55], E. Tournefier[4], S. Tourneur[39], M.T. Tran[39], M. Tresch[40], A. Tsaregorodtsev[6], P. Tsopelas[41], N. Tuning[41], M. Ubeda Garcia[38], A. Ukleja[28], A. Ustyuzhanin[63], U. Uwer[11], C. Vacca[15], V. Vagnoni[14], G. Valenti[14], A. Vallier[7], R. Vazquez Gomez[18], P. Vazquez Regueiro[37], C. Vázquez Sierra[37], S. Vecchi[16], J.J. Velthuis[46], M. Veltri[17,h], G. Veneziano[39], M. Vesterinen[11], B. Viaud[7], D. Vieira[2], M. Vieites Diaz[37], X. Vilasis-Cardona[36,p], A. Vollhardt[40], D. Volyanskyy[10], D. Voong[46], A. Vorobyev[30], V. Vorobyev[34], C. Voß[62], H. Voss[10], J.A. de Vries[41], R. Waldi[62], C. Wallace[48], R. Wallace[12], J. Walsh[23], S. Wandernoth[11], J. Wang[59], D.R. Ward[47], N.K. Watson[45], D. Websdale[53], M. Whitehead[48], J. Wicht[38], D. Wiedner[11], G. Wilkinson[55], M.P. Williams[45], M. Williams[56], H.W. Wilschut[65], F.F. Wilson[49], J. Wimberley[58], J. Wishahi[9], W. Wislicki[28], M. Witek[26], G. Wormser[7], S.A. Wotton[47], S. Wright[47], K. Wyllie[38], Y. Xie[61], Z. Xing[59], Z. Xu[39], Z. Yang[3], X. Yuan[3], O. Yushchenko[35], M. Zangoli[14], M. Zavertyaev[10,b], L. Zhang[59], W.C. Zhang[12], Y. Zhang[3], A. Zhelezov[11], A. Zhokhov[31], L. Zhong[3], A. Zvyagin[38]

1 *Centro Brasileiro de Pesquisas Físicas (CBPF), Rio de Janeiro, Brazil*
2 *Universidade Federal do Rio de Janeiro (UFRJ), Rio de Janeiro, Brazil*
3 *Center for High Energy Physics, Tsinghua University, Beijing, China*
4 *LAPP, Université de Savoie, CNRS/IN2P3, Annecy-Le-Vieux, France*
5 *Clermont Université, Université Blaise Pascal, CNRS/IN2P3, LPC, Clermont-Ferrand, France*
6 *CPPM, Aix-Marseille Université, CNRS/IN2P3, Marseille, France*
7 *LAL, Université Paris-Sud, CNRS/IN2P3, Orsay, France*
8 *LPNHE, Université Pierre et Marie Curie, Université Paris Diderot, CNRS/IN2P3, Paris, France*
9 *Fakultät Physik, Technische Universität Dortmund, Dortmund, Germany*
10 *Max-Planck-Institut für Kernphysik (MPIK), Heidelberg, Germany*
11 *Physikalisches Institut, Ruprecht-Karls-Universität Heidelberg, Heidelberg, Germany*
12 *School of Physics, University College Dublin, Dublin, Ireland*
13 *Sezione INFN di Bari, Bari, Italy*
14 *Sezione INFN di Bologna, Bologna, Italy*
15 *Sezione INFN di Cagliari, Cagliari, Italy*
16 *Sezione INFN di Ferrara, Ferrara, Italy*
17 *Sezione INFN di Firenze, Firenze, Italy*
18 *Laboratori Nazionali dell'INFN di Frascati, Frascati, Italy*
19 *Sezione INFN di Genova, Genova, Italy*
20 *Sezione INFN di Milano Bicocca, Milano, Italy*
21 *Sezione INFN di Milano, Milano, Italy*
22 *Sezione INFN di Padova, Padova, Italy*
23 *Sezione INFN di Pisa, Pisa, Italy*
24 *Sezione INFN di Roma Tor Vergata, Roma, Italy*
25 *Sezione INFN di Roma La Sapienza, Roma, Italy*
26 *Henryk Niewodniczanski Institute of Nuclear Physics Polish Academy of Sciences, Kraków, Poland*
27 *AGH - University of Science and Technology, Faculty of Physics and Applied Computer Science, Kraków, Poland*
28 *National Center for Nuclear Research (NCBJ), Warsaw, Poland*
29 *Horia Hulubei National Institute of Physics and Nuclear Engineering, Bucharest-Magurele, Romania*
30 *Petersburg Nuclear Physics Institute (PNPI), Gatchina, Russia*

[31] *Institute of Theoretical and Experimental Physics (ITEP), Moscow, Russia*

[32] *Institute of Nuclear Physics, Moscow State University (SINP MSU), Moscow, Russia*

[33] *Institute for Nuclear Research of the Russian Academy of Sciences (INR RAN), Moscow, Russia*

[34] *Budker Institute of Nuclear Physics (SB RAS) and Novosibirsk State University, Novosibirsk, Russia*

[35] *Institute for High Energy Physics (IHEP), Protvino, Russia*

[36] *Universitat de Barcelona, Barcelona, Spain*

[37] *Universidad de Santiago de Compostela, Santiago de Compostela, Spain*

[38] *European Organization for Nuclear Research (CERN), Geneva, Switzerland*

[39] *Ecole Polytechnique Fédérale de Lausanne (EPFL), Lausanne, Switzerland*

[40] *Physik-Institut, Universität Zürich, Zürich, Switzerland*

[41] *Nikhef National Institute for Subatomic Physics, Amsterdam, The Netherlands*

[42] *Nikhef National Institute for Subatomic Physics and VU University Amsterdam, Amsterdam, The Netherlands*

[43] *NSC Kharkiv Institute of Physics and Technology (NSC KIPT), Kharkiv, Ukraine*

[44] *Institute for Nuclear Research of the National Academy of Sciences (KINR), Kyiv, Ukraine*

[45] *University of Birmingham, Birmingham, United Kingdom*

[46] *H.H. Wills Physics Laboratory, University of Bristol, Bristol, United Kingdom*

[47] *Cavendish Laboratory, University of Cambridge, Cambridge, United Kingdom*

[48] *Department of Physics, University of Warwick, Coventry, United Kingdom*

[49] *STFC Rutherford Appleton Laboratory, Didcot, United Kingdom*

[50] *School of Physics and Astronomy, University of Edinburgh, Edinburgh, United Kingdom*

[51] *School of Physics and Astronomy, University of Glasgow, Glasgow, United Kingdom*

[52] *Oliver Lodge Laboratory, University of Liverpool, Liverpool, United Kingdom*

[53] *Imperial College London, London, United Kingdom*

[54] *School of Physics and Astronomy, University of Manchester, Manchester, United Kingdom*

[55] *Department of Physics, University of Oxford, Oxford, United Kingdom*

[56] *Massachusetts Institute of Technology, Cambridge, MA, United States*

[57] *University of Cincinnati, Cincinnati, OH, United States*

[58] *University of Maryland, College Park, MD, United States*

[59] *Syracuse University, Syracuse, NY, United States*

[60] *Pontifícia Universidade Católica do Rio de Janeiro (PUC-Rio), Rio de Janeiro, Brazil, associated to [2]*

[61] *Institute of Particle Physics, Central China Normal University, Wuhan, Hubei, China, associated to [3]*

[62] *Institut für Physik, Universität Rostock, Rostock, Germany, associated to [11]*

[63] *National Research Centre Kurchatov Institute, Moscow, Russia, associated to [31]*

[64] *Instituto de Fisica Corpuscular (IFIC), Universitat de Valencia-CSIC, Valencia, Spain, associated to [36]*

[65] *KVI - University of Groningen, Groningen, The Netherlands, associated to [41]*

[66] *Celal Bayar University, Manisa, Turkey, associated to [38]*

[a] *Universidade Federal do Triângulo Mineiro (UFTM), Uberaba-MG, Brazil*

[b] *P.N. Lebedev Physical Institute, Russian Academy of Science (LPI RAS), Moscow, Russia*

[c] *Università di Bari, Bari, Italy*

[d] *Università di Bologna, Bologna, Italy*

[e] *Università di Cagliari, Cagliari, Italy*

[f] *Università di Ferrara, Ferrara, Italy*

[g] *Università di Firenze, Firenze, Italy*

[h] *Università di Urbino, Urbino, Italy*

[i] *Università di Modena e Reggio Emilia, Modena, Italy*

[j] *Università di Genova, Genova, Italy*

[k] *Università di Milano Bicocca, Milano, Italy*

[l] *Università di Roma Tor Vergata, Roma, Italy*

[m] *Università di Roma La Sapienza, Roma, Italy*

[n] *Università della Basilicata, Potenza, Italy*

[o] *AGH - University of Science and Technology, Faculty of Computer Science, Electronics and Telecommunications, Kraków, Poland*

[p] *LIFAELS, La Salle, Universitat Ramon Llull, Barcelona, Spain*

[q] *Hanoi University of Science, Hanoi, Viet Nam*

[r] *Università di Padova, Padova, Italy*

[s] *Università di Pisa, Pisa, Italy*

[t] *Scuola Normale Superiore, Pisa, Italy*

[u] *Università degli Studi di Milano, Milano, Italy*

[v] *Politecnico di Milano, Milano, Italy*